Supplementary Information: Investigation of interfacial charge-carrier dynamics, degradation, and recombination mechanisms in single-junction perovskite solar cells with NiO_x and SAM hole-transporting layers via steady-state drift-diffusion model simulations

December 30, 2025

Ivona Kafedjiska[*,1,4], Vincent Le Corre[2], Hans Kobler[3,4], Igal Levine[4], Rutger Schlatmann[1,4,5] and Iver Lauermann[1,4]

[1] Helmholtz-Zentrum Berlin für Materialien und Energie GmbH, Competence Centre for Photovoltaics (PVcomB), Schwarzschildstraße 3, 12489 Berlin

[2]Mads Clausen Institute, Center for Advanced Photovoltaics and Thin Film Energy Devices (SDU CAPE), University of Southern Denmark, 6400 Sonderborg, Denmark

[3] Helmholtz-Zentrum Berlin für Materialien und Energie, Department Active Materials and Interfaces for Stable Perovskite Solar Cells, Albert-Einstein-Straße 16, 12489 Berlin

[4] Helmholtz-Zentrum Berlin für Materialien und Energie GmbH, Division Solar Energy, Kekuléstraße 5, 12489 Berlin, Germany

[5] Faculty 1 - Energy and Information, Hochschule für Technik und Wirtschaft Berlin, Germany;

[*]Corresponding author: ivona.kafedjiska@helmholtz-berlin.de

1 Choice of parameters for the simulations

All of the input parameters are listed below. The input parameters obtained from literature are color coded with orange, and those obtained via experimental measurements are color coded with green. The input parameters are generally separated into seven categories: 1) general (includes temperature; thickness of the simulated stack; VBM, CBM, and N_c of the perovskite); 2) electron and hole mobilities in the perovskite; 3) contacts (their work functions and surface recombination of the electrons and holes at the electrodes); 4) transport layers (thickness, density of states, doping, interface transfer velocity, VBM, and CBM); 5) Ions; 6) generation rates of electron-hole pairs; and 7) trapping (bulk and surface traps, and if needed, grain boundaries). The effect of the grain boundaries was disabled (set to 0).

Notice that most of the parameters were not altered as the cells were aged, except for the generation rate, the trap densities (bulk and interface) and up to an extent, the mobilities (mostly for fine-tuning of the FF and only for the samples with NiO_x(+SAM)).

HTL Type	NiOx		NiOx:Cu		NiOx + SAM		NiOx:Cu + SAM		
With respect to the aging procedure	Before	After	Before	After	Before	After	Before	After	Obtained From
T [K]	295								External Condition
L [m]	643e-9								Experimental (thickenss is controlled during deposition)
ε_r	22								Literature
CB_pero [eV]	4.47		3.87		4.27		4.17		Experimentally measured (UPS)
VB_pero [eV]	6.1		5.5		5.9		5.8		
Nc [m^-3]	6.5e23								Literature
n_0 [m^-3]	0								n.a.
p_0 [m^-3]									
mun_0 [m^2/Vs]	17e-5	1.1E-04	1.0E-04	1.0E-04	1.7E-04	1.1E-04	1.3E-04	1.3E-04	Literature & then slightly fine tuned
mup_0 [m^2/Vs]	17e-5	1.1E-04	1.0E-04	1.0E-04	1.7E-04	1.1E-04	1.3E-04	1.3E-04	
mob_n_dep	0 (constant, field-independent)								n.a.
mob_p_dep									
gamma_n									
gamma_p									
W_Left Electrode [eV]	4.52		4.05		4.43		4.32		Literature, and then adjusted in agreement with the shifts in the perovskite
W_Right Electrode [eV]	5.52		5.4		5.76		5.73		
Sn_L [m/s]	Turned off								n.a.
Sp_L [m/s]									
Sn_R [m/s]									
Sp_R [m/s]									
L_C60 [m]	23e-9								Experimental (thickenss is controlled during deposition)
L_HTL (NiO or NiO:Cu) [m]	20e-9								
Nc_C60 [m^-3]	1e26								Literature
Nc_HTL [m^-3]	1e24								
doping_C60 [m^-3]	0.0E+00								n.a.
doping_HTL [m^-3]	2e23		1.0E+22		2e23		1e22		Experimental (Hall)
mob_C60 [m^2/Vs]	1e-6								Literature
mob_HTL [m^2/Vs]	7e-6								
nu_int_C60 [m/s]	1.0E+03								

nu_int_HTL [m/s]	1.0E+03								Literature
ε_r_C60	5								
ε_r_HTL	10								
CB_C60 [eV]	4.36		4.045		4.415		4.3		Literature as starting point, and then adjusted accordingly due to the shifts caused by the HTLs in the perovskite (and then the ETL)
CB_HTL [eV]	2.14		1.85		2.28		2.17		Experimental
VB_C60 [eV]	6.36		6.045		6.415		6.3		+2 eV from CB
VB_HTL [eV]	5.74		5.45		5.78		5.77		+3.6 eV from CB
TLsAbsorb	0.0E+00								Literature
TLsTrap									
IonsInTLs									
CNI [m^-3]	5e21		2.5e21		1.0E+21		1.0E+21		
CPI [m^-3]									
mob_ion_spec	0, meaning that both positive and negative ions can be mobile species								
ion_red_rate	1								
Gehp	2.28E+27	2.29E+27	2.18E+27	2.16E+27	2.36E+27	2.24E+27	2.34E+27	2.21E+27	Experimental
Gfrac	1								Literature
Gen_profile	none								
Field_dep_G	0 (field-independent)								
P0									
Charge Sep. Distance [m]	1.0e-9								
ThermLengDist	2, meaning that the distribution is Gaussian								
Decay Rate [1/s]	1e6								
kdirect [m^3/s]	1e-17								
Lang_pre	1								
UseLangevin	0								
Bulk Trap Density [m^-3]	9.0E+19	3.2E+21	1.1E+20	3.0E+20	3.0E+20	3.0E+20	1.1E+20	9.0E+20	Experimental
Interface Trap Density_C60 [m^-2]	5.0E+14								Literature
Interface Trap Density_HTL [m^-2]	4.0E+13	1.2E+13	7.0E+13	6.5E+13	3.0E+13	2.0E+13	8.0E+13	1.2E+14	Experimental, but reported already in [3]
num_GBs	0								
GB_TrapDenisty [m^-2]	1e15		1e13				7e13		Literature. Slight fine-tuning for some of the parameters to improve the fit, if needed
Cn [m^3/s]	1e-14								
Cp [m^3/s]									
Etrap [eV]	5.3		4.7		5.0				
BulkTrapFile	none								
IntTrapFile									
Trap_type_C60	0 (neutral)								
Trap_type_HTL									
Trap_type_Bulk-and-GB	1 (donor)								

Figure 1: *All of the input parameters used in the simulations. The literature values were retrieved from [1–6].*

Elaboration on how the values for C_{60} are adjusted: The electronic changes caused by the HTL continue to impact the rest of the device and they do not end at the HTL or the perovskite bulk. Thus, while the VBM and the CBM of the C_{60} are not per se calculated or measured, they are fine tuned in line with the values for the VBM and CBM of the HTL + perovskie configuration. As a starting point, for the VBM of the C_{60} we use 6.0 eV, in line with literature.

The VBM of the perovskite with NiO_x:Cu was measured to be 5.5 eV and the VBM of the perovskite with NiO_x:Cu and NiO_x + SAM were measured to be 5.8 and 5.9 eV, respectively. So, the difference / shift in the band alignment with moving from NiO_x:Cu to NiO_x:Cu + SAM and NiO_x + SAM is 0.3 and 0.4 eV, respectively.

Then, we set the VBM of C_{60} at 6.0 eV for all of these three cells as a starting point. The best fit was obtained for the cells with NiO_x:Cu (slightly fine tuned to 6.04 eV). Then the VBM of the C_{60} for the cells with NiO_x:Cu + SAM and NiO_x + SAM was raised by 0.3 and 0.4 eV, respectively -

up to 6.3 eV (NiO_x:Cu + SAM) and 6.41 eV (NiOx + SAM) - both of which led to a good fit. The CBM is calculated by using a E_g of 2 eV.

The cells with NiO_x were an exception to this logic though. As the VBM of the perovskite with NiO_x (6.1 eV) is 0.6 eV higher than the VBM of the perovskite with NiO_x:Cu (5.5 eV), one would expect a 0.6 eV shift in the VBM of the C_{60} as well (6.6 eV). However, this did not lead to a good fit of the JV curve, so the VBM was gradually decreased, until the value converged at 6.36 eV. This indicates that the sub-optimal band alignment at the NiO_x-perovskite interface, affects the band alignment at the ETL-perovskite interface as well.

The doping and the mobility in the HTL were obtained from Hall measurements for NiO_x(:Cu) and it was assumed that passivating the NiO_x(:Cu) surface with SAM does not change the doping in the bulk of the NiO_x(:Cu) (*Figure 2*).

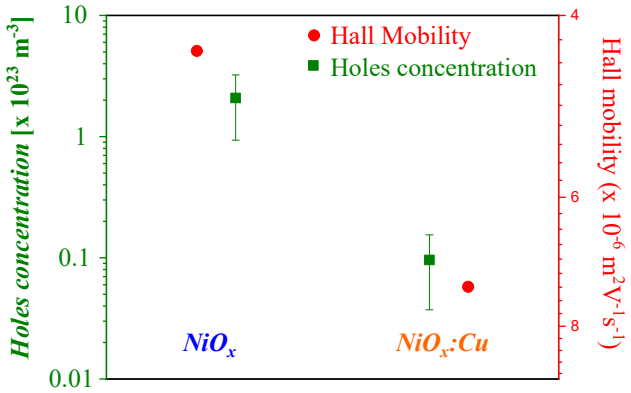

Figure 2: *Hall measurements for the concentration of holes in NiO_x and NiO_x:Cu. The extracted values for the simulations are written in Table 1 above.*

2 JV Curves: Aging Experiments and Varying Scan Speeds

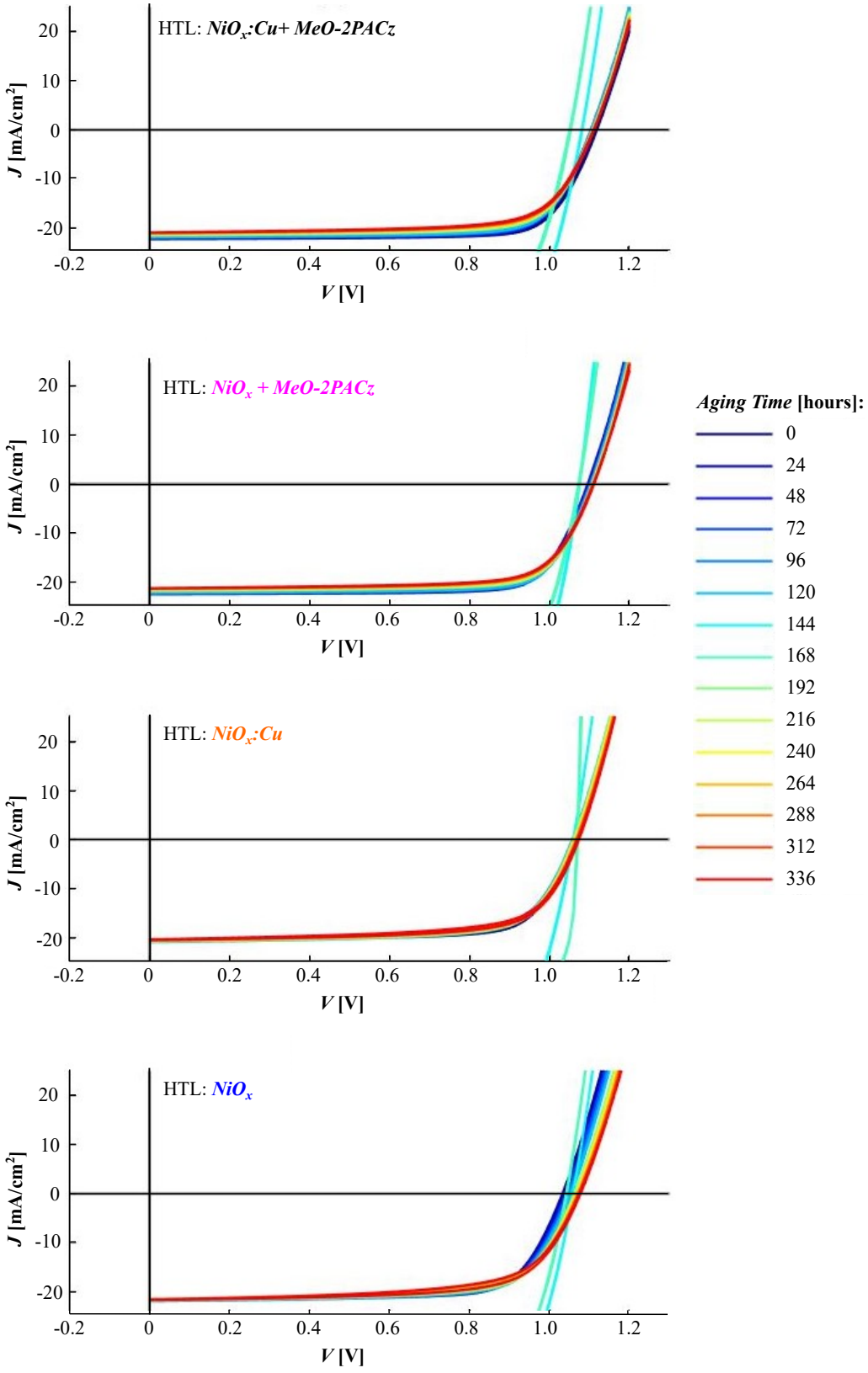

Figure 3: *The JV curves of the champion devices per HTL with respect to stability. The simulated JV curves in Figure 1 in the paper are taken at aging times of 0 hours (fresh) and at 336 hours (14-days aged cells). The electrical contact to the cells was lost on the seventh and eighth day (144 and 168 hours), causing an artifact in the JV curves. The measurements continued upon fixing this issue.*

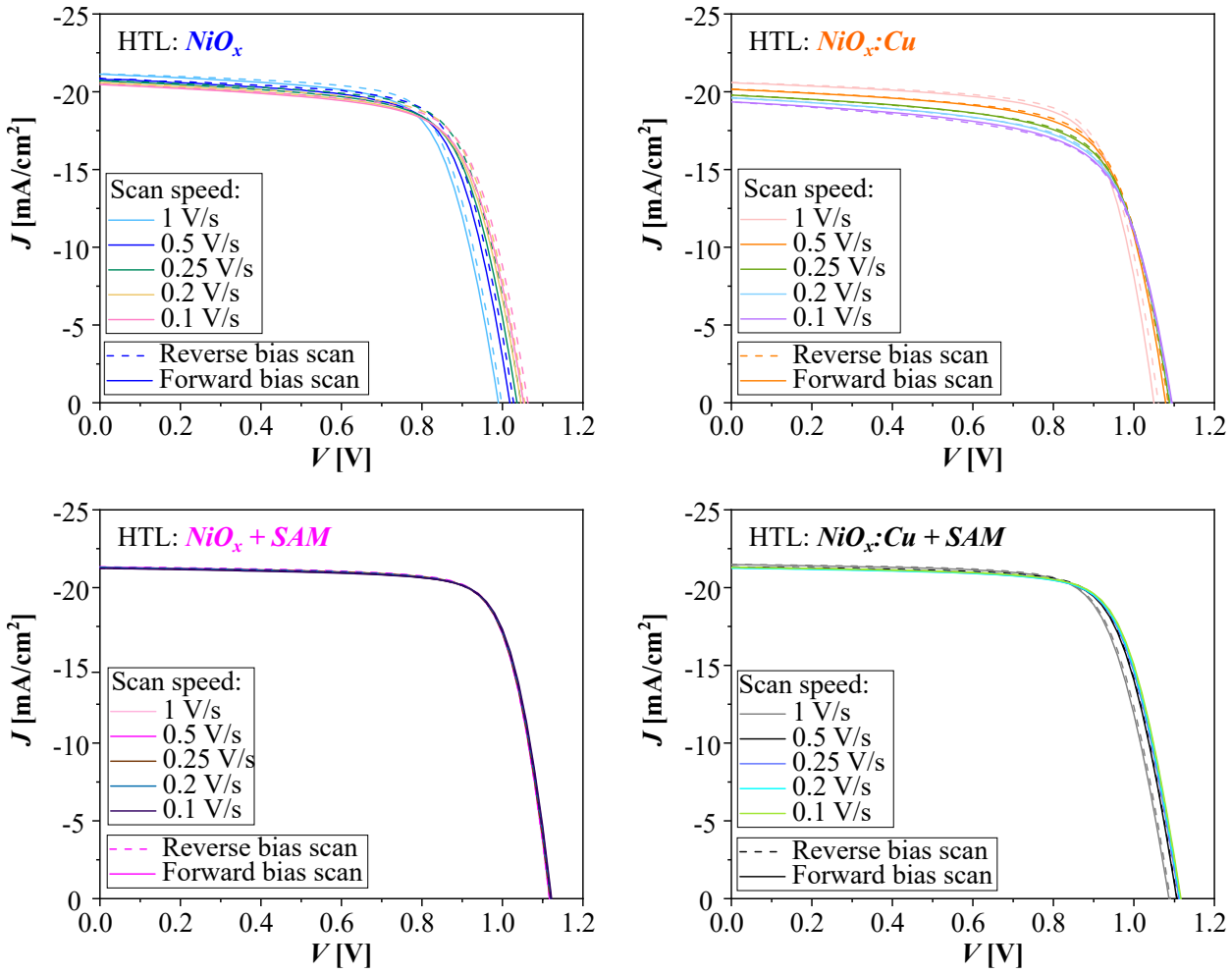

Figure 4: *One averaged JV curve per scan rate from the six pixels on a given sample for each HTL: NiO_x, NiO_x:Cu, NiO_x + SAM, NiO_x:Cu + SAM. The hysteresis factors presented in Figure 7 in the paper were obtained from these JV curves.*

3 Traps' densities and rates of recombination

	NiO_x		NiO_x:Cu		NiO_x + SAM		NiO_x:Cu + SAM	
	Fresh	Aged	Fresh	Aged	Fresh	Aged	Fresh	Aged
$\mathbf{Traps}_{HTL-pero}$ $\times 10^{13}$ m^{-2}	4.0	1.2	7.0	6.5	3.0	2.0	8.0	12.0
$\mathbf{Traps}_{Bulk}$ $\times 10^{20}$ m^{-3}	0.9	32.1	1.1	3.0	3.0	3.0	1.1	9.0
$\mathbf{R}_{dir}$ $\times 10^{23}$ m^{-3}/s	0.07	0.19	6.99	6.84	3.46	0.08	7.83	3.37
$\mathbf{R}_{Bulk-SRH}$ $\times 10^{25}$ m^{-3}/s	0.01	0.03	3.17	8.46	9.21	0.06	2.34	5.23
$\mathbf{R}_{Int-SRH-n}$ $\times 10^{28}$ m^{-3}/s	198.25	206.54	3.18	2.89	1.48	130.17	1.46	1.09
$\mathbf{R}_{Int-SRH-p}$ $\times 10^{28}$ m^{-3}/s	0.002	0.001	0.26	0.24	0.01	0.01×10^{-2}	0.24	0.18

Table 1: *Holes trap density at the HTL-perovskite interface ($Traps_{HTL-pero}$) and in the perovskite bulk ($Traps_{Bulk}$) followed by varying rates of recombination at V_{oc} for fresh and aged single-junction perovskite solar cells with NiO_x(:Cu)(+SAM) HTLs and C_{60}-SnO_2 as an ETL stack. R_{dir}: direct recombination; $R_{Bulk-SRH}$: recombination via bulk traps; $R_{Int-SRH-n}$ or $R_{Int-SRH-p}$: recombination via interface traps, where n and p distinguish between trapping of electrons and holes, respectively.*

4 UPS Measurements

The work function (WF, see *Figure 6a*) is determined via

$$WF = h\nu - E_{SEE} - E_F, \tag{1}$$

where $h\nu$ is the excitation energy (21.2 eV), E_{SEE} is the binding-energy point where the linear extrapolation of the secondary electron edge (SEE) intercepts the background, and E_F is the shift away from 0 eV of the Fermi level of a clean gold (Au) sample contacted to both the sample and the manipulator in the analytic chamber. This calibration gives us 1.19 eV shift for the Fermi level of the gold (*Figure 6b*).

The VBM is determined by a linear extrapolation of the leading edge of the UPS spectrum until the line intercepts the pre-determined background. The error ascribed to the UPS measurements is obtained by averaging the two most extreme linear fits for the dominant linear slope and reported as the deviation between the minimum and the maximum value from this average value.

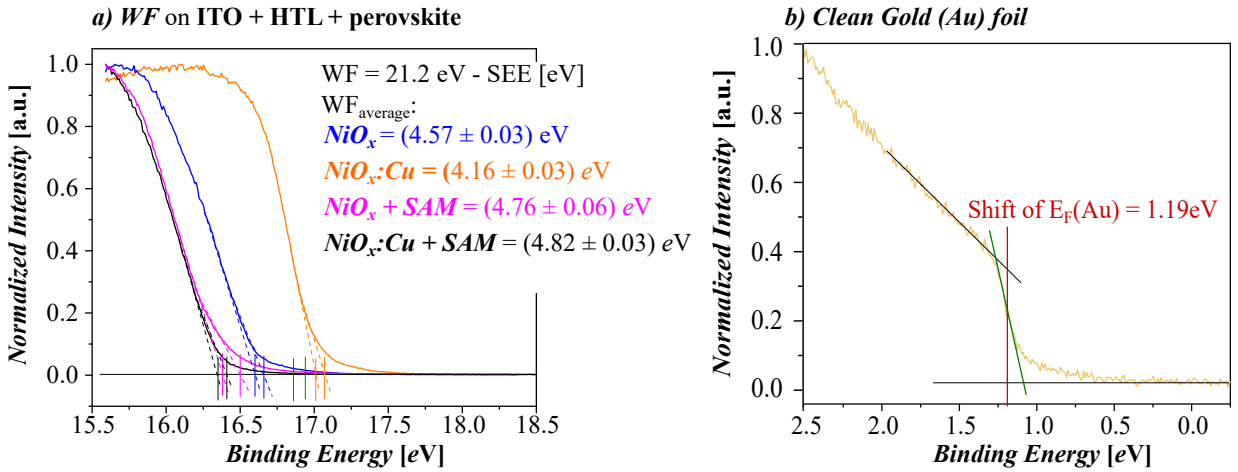

Figure 5: *a) Work function (WF) of the triple-cation perovskite films deposited and then measured on top of an ITO + HTL + perovskite partial-cell stack. The extracted value is the average of the two values denoted on the plot. The HTLs are NiO_x (blue), NiO_x:Cu (orange), NiO_x + SAM (magenta), and NiO_x:Cu + SAM (black). The SAM is MeO-2PACz. b) Calibration with a clean gold sample to find its Fermi-level shift.*

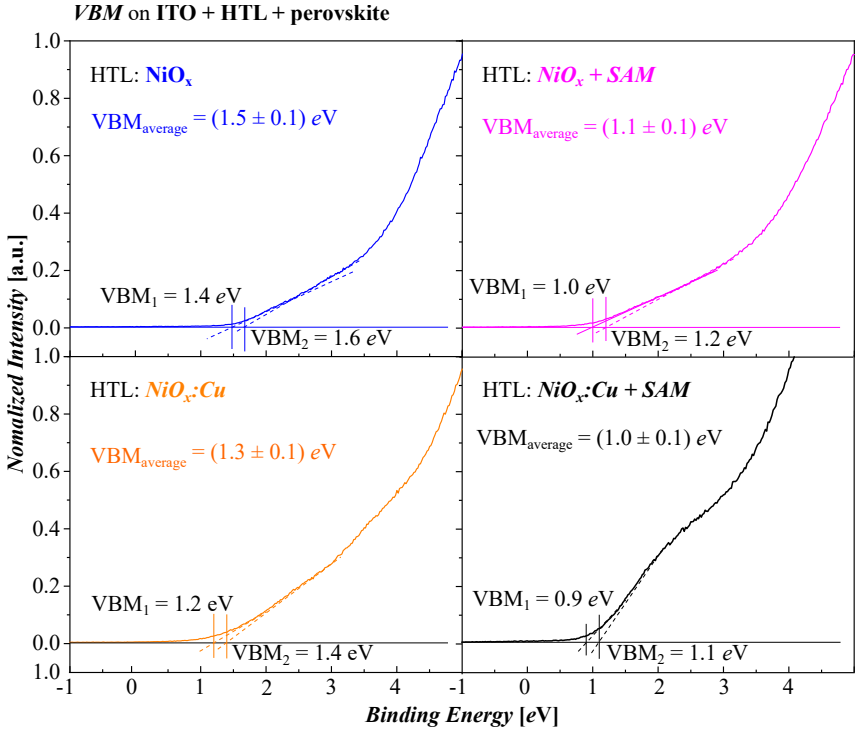

Figure 6: *Valence band maxima (VBM) of the triple-cation perovskite films deposited and then measured on top of an ITO + HTL + perovskite partial-cell stack. The HTLs are NiO_x (blue), NiO_x:Cu (orange), NiO_x + SAM (magenta), and NiO_x:Cu + SAM (black). The SAM is MeO-2PACz.*

References

[1] Vincent M. Le Corre et al. "Device Modeling of Perovskite Solar Cells: Insights and Outlooks". In: *Soft-Matter Thin Film Solar Cells*. AIP Publishing Books. AIP Publishing LLC, Sept. 2020, pp. 4–1–4–32. DOI: 10.1063/9780735422414_004.

[2] Pietro Caprioglio et al. "On the Relation between the Open-Circuit Voltage and Quasi-Fermi Level Splitting in Efficient Perovskite Solar Cells". In: *Adv. Energy Mater.* 9.33 (Sept. 2019), p. 1901631. DOI: 10.1002/aenm.201901631.

[3] Ivona Kafedjiska et al. "Advanced Characterization and Optimization of NiOx: Cu-SAM Hole-Transporting Bi-Layer for 23.4% Efficient Monolithic Cu (In, Ga) Se2-Perovskite Tandem Solar Cells". In: *Advanced Functional Materials* (), p. 2302924.

[4] Vincent M. Le Corre et al. "Quantification of Efficiency Losses Due to Mobile Ions in Perovskite Solar Cells via Fast Hysteresis Measurements". In: *Solar RRL* 6.4 (2022), p. 2100772. DOI: 10.1002/solr.202100772.

[5] Marten Koopmans and L Jan Anton Koster. "Voltage deficit in wide bandgap perovskite solar cells: the role of traps, band energies, and effective density of states". In: *Solar RRL* 6.12 (2022), p. 2200560.

[6] Albert These et al. "Beginner's Guide to Visual Analysis of Perovskite and Organic Solar Cell Current Density–Voltage Characteristics". In: *Advanced Energy Materials* 14.21 (2024), p. 2400055.